Environmental Science & Technology

pubs.acs.org/est

Article

Laboratory-Simulated Photoirradiation Reveals Strong Resistance of Primary Macroplastics to Weathering

Xiangtao Jiang, Scott Gallager, Rut Pedrosa Pàmies, S. Emil Ruff, and Zhanfei Liu*

Cite This: *Environ. Sci. Technol.* 2024, 58, 14775−14785

Read Online

ACCESS | Metrics & More | Article Recommendations | Supporting Information

ABSTRACT: The photodegradation of macroplastics in the marine environment remains poorly understood. Here, we investigated the weathering of commercially available plastics (tabs 1.3 × 4.4 × 0.16 cm), including high-density polyethylene, low-density polyethylene, polypropylene, polystyrene, and polycarbonate, in seawater under laboratory-simulated ultraviolet A radiation for 3−9 months, equivalent to 25−75 years of natural sunlight exposure without considering other confounding factors. After the exposure, the physical integrity and thermal stability of the tabs remained relatively intact, suggesting that the bulk polymer chains were not severely altered despite strong irradiation, likely due to their low specific surface area. In contrast, the surface layer (∼1 μm) of the tabs was highly oxidized and eroded after 9 months of accelerated weathering. Several antioxidant additives were identified in the plastics through low temperature pyrolysis coupled with gas chromatography/mass spectrometry (Pyr-GC/MS) analysis. The Pyr-GC/MS results also revealed many new oxygen-containing compounds formed during photodegradation, and these compounds indicated the dominance of chain scission reactions during weathering. These findings highlight the strong resistance of industrial macroplastics to weathering, emphasizing the need for a broader range of plastics with varying properties and sizes to accurately estimate plastic degradation in the marine environment.

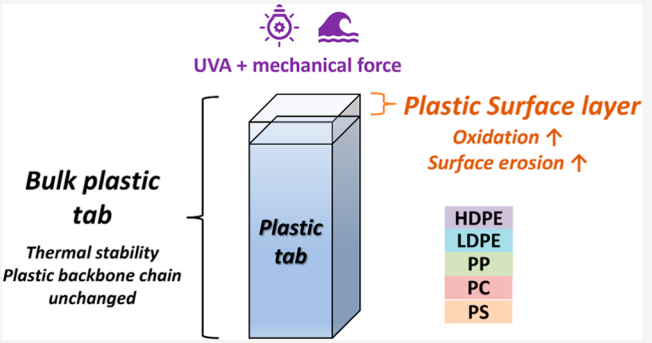

KEYWORDS: *macroplastic, photodegradation, FTIR, pyrolysis-GC/MS, additive, Norrish reactions*

INTRODUCTION

Due to a substantial rise in global plastic production annually, plastic pollution has become a major environmental concern. More than 40% of plastic waste is not properly managed, leading to an annual influx of approximately 8 million metric tons of plastic into the world's oceans,[1] although the exact influx is still under debate.[2] When exposed to various environmental stressors such as ultraviolet (UV) irradiation and mechanical forces, plastic debris undergoes degradation and thus breaks down into smaller pieces, often following a degradation path from macro- to micro- and nanosized particles.[3−5] The detrimental effects of micro- or nanosized plastics on marine organisms have been relatively well documented, including the obstruction of digestive tracks,[6] organ inflammation,[7−9] the transfer of organic pollutants,[10] and the accumulation within food chains.[11,12] These effects have potential implications for human health. Consequently, there is an urgent need to comprehend the environmental behavior of plastic debris, including its degradation and fate in marine waters.

The weathering of plastics has been studied under various environmental conditions, with evidence gathered from both field observation and laboratory simulation experiments.[13−16] For example, the increase in oxygen content or oxygen-containing functional groups of plastic particles has been reported following UV exposure, typically in a few months,[17] while deterioration of plastic surface properties, such as discoloration, cracks, and fragments, is often observed from plastic debris collected in the field.[18] The processes of plastic weathering under different environmental conditions have been categorized and summarized.[3,4,19] As a key process in plastic weathering, photodegradation involves reactions between free radicals and plastic carbon chains, leading to oxidation, chain scission, and/or cross-linking of the carbon chains, which alter the molecular structure of polymers.[20−23] The presence of molecular oxygen during photodegradation fosters the formation of peroxides and carbonyl compounds, resulting in changes in material properties and possible fragmentation with mechanical forces.[24−26] Understanding

Received: November 25, 2023
Revised: July 3, 2024
Accepted: July 5, 2024
Published: August 6, 2024

these processes is crucial for comprehending the environmental degradation of plastics and their potential impacts.

Currently, research on the weathering process of plastics has been directed more toward polyolefins and polystyrene,[4] primarily through examining micro- and nanosized plastic particles or thin films, due to their widespread production and ease of synthesis, with less studies using other materials.[27] While many earlier studies used pure polymer materials to ensure controlled and reproducible conditions, an increasing number of recent studies have started investigating the weathering of commercial plastics commonly used in daily life.[28] Commercial plastic products are environmentally realistic, although their higher complexity concerning polymer type, shape, size, thickness, and the presence of additives can influence the weathering processes.[29,30] Moreover, different environmental conditions, including UV exposure, intensity, abrasion, wave action, dissolved organic matter concentrations, and fluctuations in temperature, can significantly impact the rate of plastic weathering. Furthermore, the quantification of plastic weathering rates has received limited attention, with carbonyl moieties measured through spectral instruments being the primary metric, which has limitations, particularly regarding plastic size and flatness.[29,31]

To address these knowledge gaps, we conducted photodegradation experiments using commercially available macroplastics under laboratory-simulated coastal conditions. The surface chemistry, morphology, thermal stability, and additive composition of the plastics were characterized using a suite of analytical tools, including conventional characterization instruments such as Fourier transform infrared spectroscopy (FTIR), scanning electron microscopy (SEM), thermogravimetric analysis (TGA), chemical characterization techniques, and pyrolysis gas chromatography−mass spectrometry (Pyr-GC/MS). Our overall goal was to gain a thorough understanding of how commercial macroplastics are photo- and mechanically degraded in seawater under long-term UV exposure.

MATERIALS AND METHODS

Materials. High-density polyethylene (HDPE), low-density polyethylene (LDPE), polypropylene (PP), polystyrene (PS), and polycarbonate (PC) plastic sheets, as the primary plastic without weathering previously, were obtained from McMaster-Carr Supply Company (USA). These polymers were chosen because of their large-scale global production and their widespread presence in the marine environment.[32] The plastic sheets (122 cm × 61 cm) had a thickness of 1.6 mm. The exact formula and additive information were not provided by the vendor. However, plastic additives in various concentrations were confirmed in different plastics through Pyr-GC/MS (details in Supporting Information and Figure S1). Plastic sheets were cut into small tabs (1.3 cm × 4.4 cm) and then cleaned with DI water and dried in a laminar-flow hood before further use.

Weathering Experiment. To simulate long-term weathering conditions in the marine environment, plastic tabs underwent a controlled experimental setup. Four plastic tabs of each polymer type were placed within a 10 cm Pyrex crystallizing dish filled with 200 mL of filtered natural seawater (1 μm spiral wound cartridge filter, Pall, USA, salinity 32 psu) and maintained at 55 °C with three replicates. Additionally, approximately 10,000 glass beads (1 mm diameter) were introduced to the dish, covering 80% of the dish's bottom surface area, with continuous agitation provided by a rotary table (stroke length 10 cm, speed 60 rpm) to simulate the effects of physical contact with sediment particles in coastal water. UVA lighting (315−400 nm) was applied using three overhead LED UV lamps (Isuerfy, 120 W, F120W-UV-US), positioned 3 cm above the dishes, with an intensity of 230 W/m^2 each, verified by a UV light meter (UV513AB, General Tools). UVA was selected due to its prevalence and deeper penetration depth over the other UV bands.[33,34] On average, the simulated UVA irradiance was approximately 50 times that of natural UVA strength, estimated at 4.5 W/m^2 reaching the earth on a global average,[35] i.e., 3 months of continuous light exposure in this experiment equals approximately 25 years of natural diel UVA exposure in the ocean. To maintain constant salinity and water levels, distilled water was replenished every other day.

The plastic tabs were subsampled at four different time points: T_0 (before weathering), T_1 (3 months ≈ 25 years), T_2 (6 months ≈ 50 years), and T_3 (9 months ≈ 75 years). These time points were chosen to capture the progressive changes in the plastic tabs over the course of the weathering process. The experimental design, involving the coincubation of plastic tabs of the same polymer with agitation, posed challenges for tracking the weight change of a specific tab at a given time point. Additionally, due to incubation in seawater, effectively removing all sea salt adhered to the plastic surface through water rinsing was difficult. Thus, we did not measure the weight loss of the tabs with the exposure time.

Measurements. *FTIR.* The extent of weathering on the surface of plastic tabs was assessed by an FTIR instrument (IRTracer-100, Shimadzu) equipped with an attenuated total reflectance (ATR) accessory. The FTIR spectra were recorded in the range of 4000 to 700 cm^{-1} at a resolution of 8 cm^{-1}, averaging 32 scans. To scale the spectra within a similar range, the obtained spectra were first baseline corrected and then normalized using LabSolution software (Shimadzu) by setting the minimum value to zero and scaling the maximum absorption value to 100%. For each plastic tab, six replicate measurements were performed on randomly selected areas (on both sides of the tab).

Newly formed functional groups, including hydroxyls, carbonyls, and vinyl (alkenes), were identified and used for characterizing the weathering degree of plastic tabs.[17,36] An oxidation index was calculated to assess the surface oxidation of the plastic tabs. The oxidation index for each polymer was determined by summing four individual bonds: R−OH (alcohol),[17] C−O (ether),[17] C═O (ketone),[17,36] and C═C (vinyl).[17] The indices were calculated by comparing the maximum absorbance value of the corresponding peak to the value of a reference peak specific to each polymer. The specific equations used to calculate the indices are as follows:

$$\text{R−OH index} = A\_(3300 - 3400)/A\_\text{plastic}$$

$$\text{C−O index} = A\_(1100 - 1200)/A\_\text{plastic}$$

$$\text{C═O index} = A\_(1690 - 1730)/A\_\text{plastic}$$

$$\text{C═C index} = A\_(1620 - 1650)/A\_\text{plastic}$$

where A stands for maximum peak absorbance among different wavelength ranges. The reference plastic peaks were 2908−2920 cm^{-1} for PE, 2885−2940 cm^{-1} for PP, 1771 cm^{-1} for PC, and 2851 cm^{-1} for PS.[4,19,37]

SEM. The surface morphology of the plastic tabs was examined using a JEOL SEM. Plastic tabs were cut to a size of

https://doi.org/10.1021/acs.est.3c09891
Environ. Sci. Technol. 2024, 58, 14775−14785

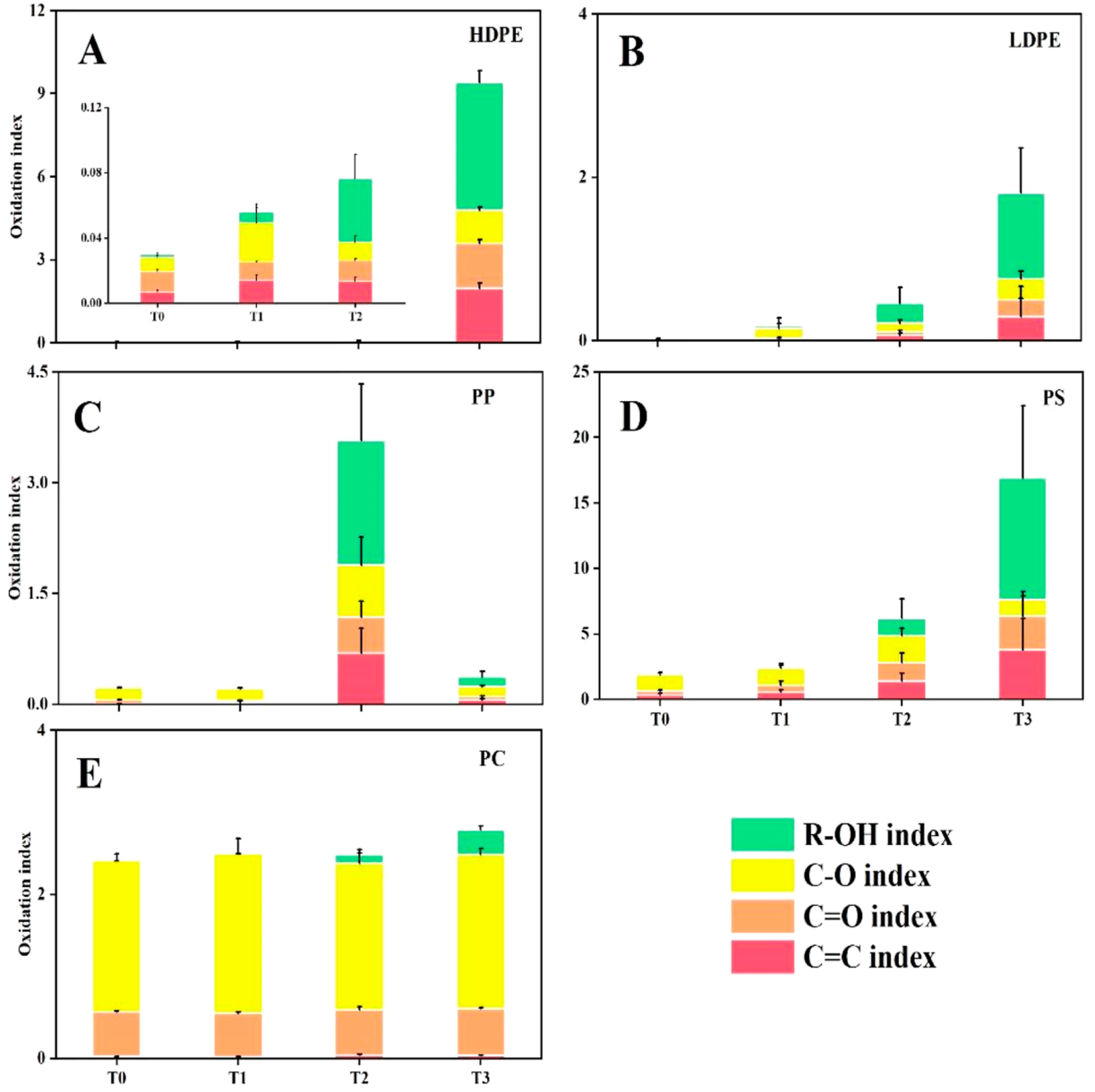

Figure 1. Oxidation indices of HDPE (A), LDPE (B), PP (C), PS (D), and PC (E) from laboratory weathering experiments. T_0-T_3 represents 0–9 months of weathering, and indices of different functional groups were from the FTIR analysis. Data are the averages of six replicate measurements; error bars represent the standard deviations.

0.6 × 0.6 cm using rinsed stainless-steel scissors. The samples were then placed on double-sided carbon tape and coated with 15 nm of gold powder to enhance conductivity. The SEM was operated at 12 kV under high vacuum, with magnifications ranging from 25 to 500×, which allowed for a detailed examination of the surface appearance and any possible changes resulting from weathering. For each individual sample, four images were captured, and the image with the best resolution for each magnification was selected and reported.

TGA. TGA was performed using a thermogravimetric analyzer (Shimadzu TGA-50) under a nitrogen atmosphere (50 mL/min flow rate) with three replicates for each polymer type. Briefly, the plastic tabs were cut into small pieces, and a sample weighing 5–10 mg was analyzed. The sample in a platinum pan was heated from 30 to 650 °C at a rate of 5 °C/min. TG and derivative TG (DTG) curves were recorded to assess the thermal behavior of the sample. The TG onset temperatures (T_{onset}), defined as a 3% (w/w) loss, and the DTG maximum temperatures (T_{max}) were calculated from the curve to determine the thermal stability of the plastic, following the method described by Yamada et al.[38]

Pyr-GC/MS. Pyrolysis analysis was conducted using a multishot pyrrolyzer (EGA/Py-3030D, Frontier Laboratories Ltd.) coupled with a GC/MS system (Shimadzu GCMS-TQ8040). To monitor potential cross-contamination, sample carryover, and instrument-related contamination, each sample run was followed by three blank runs before the next sample. A tab subsample, weighing 2–5 mg, was randomly cut by rinsed metal scissors and placed in a pyrolyzer cup. Two temperature modes were applied: high temperature (600 °C for 0.3 min, as detailed in Supporting Information) and low temperature (350 °C for 0.3 min) pyrolysis modes. For the low temperature mode, the GC inlet temperature was set at 300 °C, and the split ratio was 5:1. An Ultra ALLOY Capillary Column UA+-5

https://doi.org/10.1021/acs.est.3c09891
Environ. Sci. Technol. 2024, 58, 14775−14785

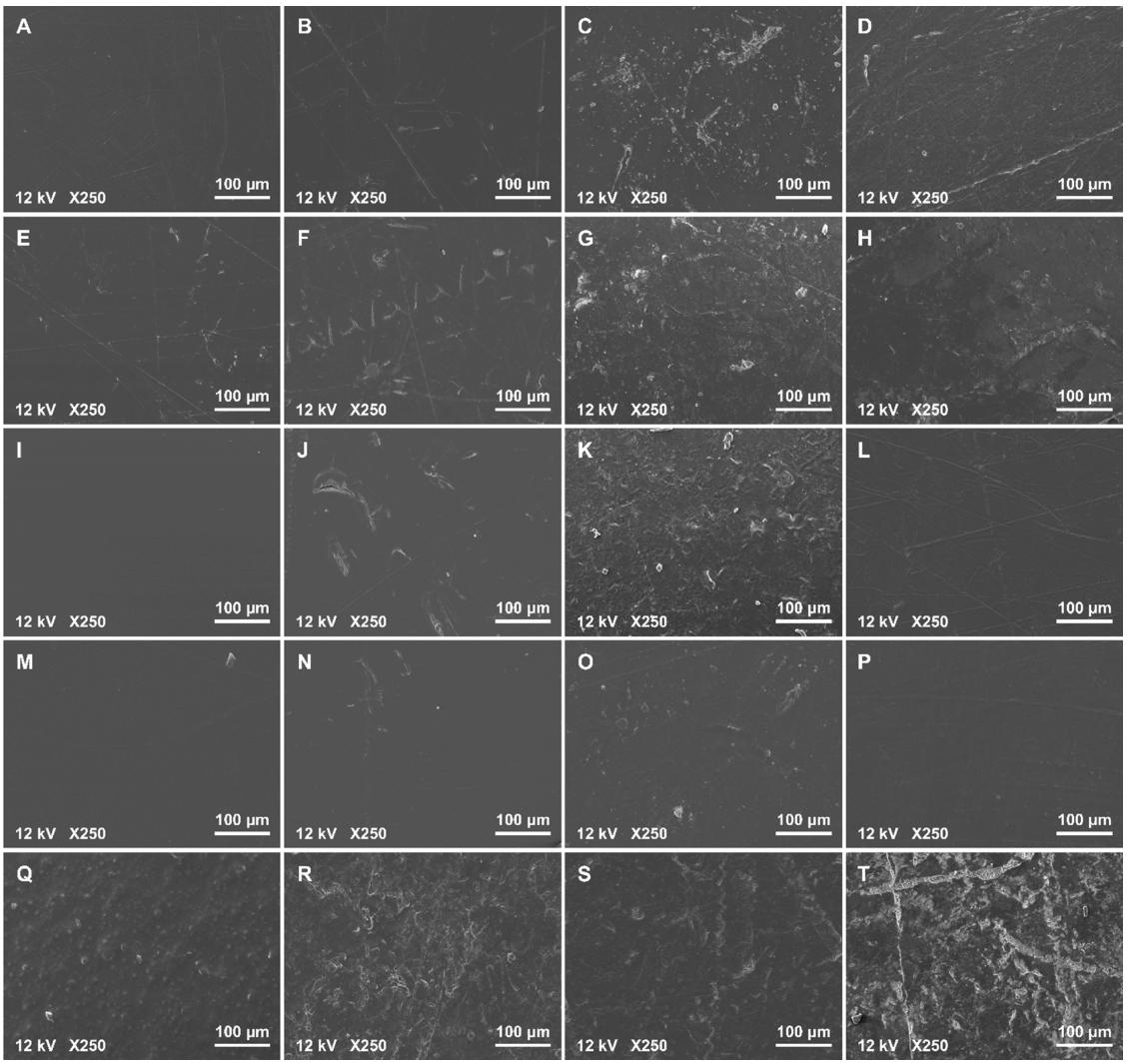

Figure 2. SEM images of surface morphology with magnification of 250× by increasing weathering exposure days for HDPE (A,B,C,D at T_0, T_1, T_2, and T_3, respectively), LDPE (E,F,G,H at T_0, T_1, T_2, and T_3, respectively), PC (I,J,K,L at T_0, T_1, T_2, and T_3, respectively), PP (M,N,O,P at T_0, T_1, T_2, and T_3, respectively), and PS (Q,R,S,T at T_0, T_1, T_2, and T_3, respectively).

(30 m length, 0.25 mm I.D., and 0.25 μm film thickness consisting of 95% polydimethylsiloxane and 5% polydiphenyldimethylsiloxane stationary phase, Frontier Laboratories Ltd.) was employed, with helium as the carrier gas at a flow rate of 1 mL/min. The GC oven program was set as follows: 50 °C (hold 1 min) → 8 °C/min →130 °C (hold 4 min) → 50 °C/min →320 °C (hold 5 min). Pyrolyzate chemical structures were identified by comparing them with the NIST17 library via LabSolution software (Shimadzu). Triplicate samples for each plastic type were analyzed.

RESULTS AND DISCUSSION

Photodegradation of the Plastic Surface: Insights from FTIR and SEM. The weathering of plastics typically initiates at the surface; thus, the plastic tabs in this study are ideal to interrogate the surface photodegradation processes of different plastic polymers both quantitatively and mechanistically. The insights into surface processes were gained through two techniques, FTIR and SEM. The FTIR used for this work was ATR, where total reflection occurs at the interface between germanium (Ge) and the plastic surface. The penetration depth for Ge is approximately 0.57 μm,[39] which is considerably less than the thickness of the plastic tabs (1.6 mm) used in this study. Even when analyzing both sides of the plastic tab, the information obtained was limited to the very surface layer, representing <1‰ of the entire polymer volume. Consequently, the FTIR results reflect the processes occurring in the extremely thin surface layer of the plastic tabs.

The oxidation index of different plastic types and their FTIR spectra at various UVA weathering durations are summarized in Figure 1 and Supporting Information Figure S2. All types of plastics were oxidized by irradiation, resulting in notable new peaks in their FTIR spectra at 3300−3400, 1690−1720, 1620−1650, and 1100−1200 cm^{-1}, which were assigned as ketone, ester, alcohol, and vinyl groups, respectively. In HDPE, LDPE, and PS, the oxidation indices continuously increased from 0 to 6 months of UVA exposure and then showed a steep increase after 9 months. The oxidation index of HDPE increased from 0.03 ± 0.00 at T_0 to 0.06 ± 0.02, 0.08 ± 0.02, and finally 9.40 ± 0.88 (ANOVA, n = 6, p = 0.0001) at T_1, T_2, and T_3, respectively; along the same time frame, that of LDPE increased from 0.03 ± 0.01 to 0.18 ± 0.17, 0.46 ± 0.25, and 1.80 ± 0.97 (ANOVA, n = 6, p = 0.0001), respectively. The indices of PS showed the greatest changes among all of the

https://doi.org/10.1021/acs.est.3c09891
Environ. Sci. Technol. 2024, 58, 14775−14785

Table 1. Onset and Maximum Temperatures Calculated from TGA Results of HDPE, LDPE, PP, PS, and PC at Different Laboratory Weathering Durations[a]

	T_{onset}				T_{max}			
	T_0	T_1	T_2	T_3	T_0	T_1	T_2	T_3
HDPE	439 ± 7	428 ± 2	433 ± 6	438 ± 2	478 ± 0	480 ± 3	479 ± 2	475 ± 9
LDPE	418 ± 3	415 ± 5	418 ± 3	418 ± 2	468 ± 5	470 ± 5	472 ± 4	474 ± 4
PP	394 ± 3	398 ± 7	397 ± 5	394 ± 11	449 ± 5	458 ± 1	455 ± 1	451 ± 5
PS	382 ± 6	384 ± 2	384 ± 4	384 ± 2	428 ± 10	432 ± 4	431 ± 3	433 ± 9
PC	443 ± 5	454 ± 4	442 ± 4	446 ± 8	474 ± 11	494 ± 14	478 ± 8	498 ± 4

[a]The ± data represent standard deviations of three replicate analyses.

plastics, ranging from 1.98 ± 0.13 at T_0 to 2.50 ± 1.00, 6.20 ± 1.64, and 16.90 ± 9.93 (ANOVA, $n = 6$, $p = 0.0004$) at T_1, T_2, and T_3, respectively. This pronounced increase of PS indices is likely due to its aromatic ring structure, which absorbs UV light, thus leading to more extensive photodegradation. In contrast, the changes in PC oxidation indices were not significant during the first 6 months of weathering (ANOVA, $n = 6$, $p = 0.885$), followed by a slight increase at 9 months (ANOVA, $n = 6$, $p = 0.008$) (from 2.41 ± 0.09 at T_0 to 2.50 ± 0.20, 2.48 ± 0.23, and 2.78 ± 0.09 at T_1, T_2, and T_3, respectively). The oxidation indices of PP increased slightly from 0 to 3 months, followed by a significant increase at 6 months (ANOVA, $n = 6$, $p = 0.0001$) but dropped at 9 months (from 0.22 ± 0.01 at T_0 to 0.22 ± 0.04, 3.57 ± 1.71, and 0.38 ± 0.12 at T_1, T_2, and T_3, respectively). This pattern suggests that the oxidized components on the PP surface were lost to and/or dissolved in the seawater after 6 months and thus exposed the fresher interior. This process may have been enhanced by constant agitation in the weathering chamber. Consistent with our findings, it has been often reported that the oxidation (carbonyl) index of PP shows a plateau or drop-off after a certain duration of UV exposure in photodegradation experiments.[40] This phenomenon has been attributed to the fragmentation or peeling off of the oxidized surface caused by mechanical forces or the loss of volatile oxidation products through diffusion to the ambient air or water.[41] As a result, the virgin inner part of the PP plastic is newly exposed to oxidation. However, the peeling-off or dissolution seemed to have significantly occurred only to PP but not to other types of plastics, suggesting that photodegradation products from the branch-chain PP structures are more soluble or fragile.

The changes of specific oxidation indices with time were similar among LDPE, HDPE, PP, and PS. From 0 to 3 months, the increase in the oxidation index was primarily driven by C−O and C═O bonds. However, from 3 to 9 months, the oxidation index was mainly contributed by the R−OH, while C═C played a role throughout the entire weathering process. This pattern suggests that the same oxidation mechanisms were at play for these 4 types of plastics, although the mechanisms changed with time. In contrast, only the increase in the R−OH index was pronounced for PC, while the small fluctuations in the C═O and C−O indices were not indicative of the oxidation status of the plastic since PC itself contains carbonyls.

Regarding the morphology of plastic tabs at different weathering time points, the tabs did not present discoloration based on unaided visual or microscopical observation. However, SEM images revealed changes in surface morphology with exposure duration (Figure 2). At T_0, the plastic surfaces all appeared to be smooth and uniform, except for some minor scratches, likely resulting from shipping and handling. As weathering progressed, the surfaces of HDPE, LDPE, and PS showed cracks and rugged textures and the presence of small fragments. In contrast, the surface deterioration of PC and PP was more prominent after 6 months, with the most notable "wear and tear". Surprisingly, the surfaces of PC and PP plastics appeared smoother at 9 months, indicating a possible loss of oxidized plastic surface through embrittlement, flaking off, or dissolution in seawater, consistent with the FTIR data discussed above. However, PC did not fully follow these oxidation index variations, possibly due to its oxygen-containing backbone.

Photodegradation of Bulk Plastics as Indicated by TGA and Pyr-GC/MS. The subsamples of plastic tabs for TGA and Pyr-GC/MS analyses included both the surface and inner parts of a tab; thus, the results reflect changes of the bulk plastics. TG and DTG curves were recorded in Figure S3. The thermal stability of all plastics remained relatively constant throughout the weathering duration (Table 1), including both the onset temperature (T_{onset}) and the maximum temperature (T_{max}). For example, the T_{onset} of HDPE varied from 439 ± 7 at T_0 to 428 ± 2, 433 ± 6, and 438 ± 2 °C at T_1, T_2, and T_3, respectively (ANOVA, $n = 3$, $p = 0.19$); the T_{max} of HDPE fluctuated slightly from 478 ± 0 at T_0 to 480 ± 3, 479 ± 2, and 475 ± 9 °C at T_1, T_2, and T_3, respectively (ANOVA, $n = 3$, $p = 0.82$). Even though significant chemical and physical changes occurred on the plastic surface from FTIR and SEM analyses, the overall structure and thermal stability of the main backbone chain remained relatively unchanged following the intensive UVA exposure. In addition, the residues of all plastics except PC were <4% by weight after the TGA analysis, indicating a very small amount of inorganic additives, if any, normally titanium dioxide or calcium carbonate.[28] In contrast, residues of PC after TGA accounted for 20% in coke form, which may be due to its high oxygen and aromatic content, facilitating the formation of graphite.[42]

Pyr-GC/MS was applied to evaluate the effects of weathering on the chemical composition of the plastics at the molecular level. Traditional high-temperature pyrolysis (e.g., 600 °C, 0.3 min) was first applied to the plastic tabs at different weathering stages (results in Supporting Information). The pyrolyzates were dominated by cracking products from the plastic backbone, while the oxidation products of plastics were undetectable (Figure S4). However, there was a clear difference in the overall GC chromatograms before and after weathering, i.e., the proportion of certain peaks over the total. For example, the percentage of *n*-alkane C_{13-23} from HDPE increased with weathering time (from 48.9% at T_0 to 50.4, 52.2, and 53.69% at T_1, T_2, and T_3, respectively; Figure S4F). This increase might be attributed to the photooxidation of HDPE, which introduces oxygen into the polymer carbon

https://doi.org/10.1021/acs.est.3c09891
Environ. Sci. Technol. 2024, 58, 14775−14785

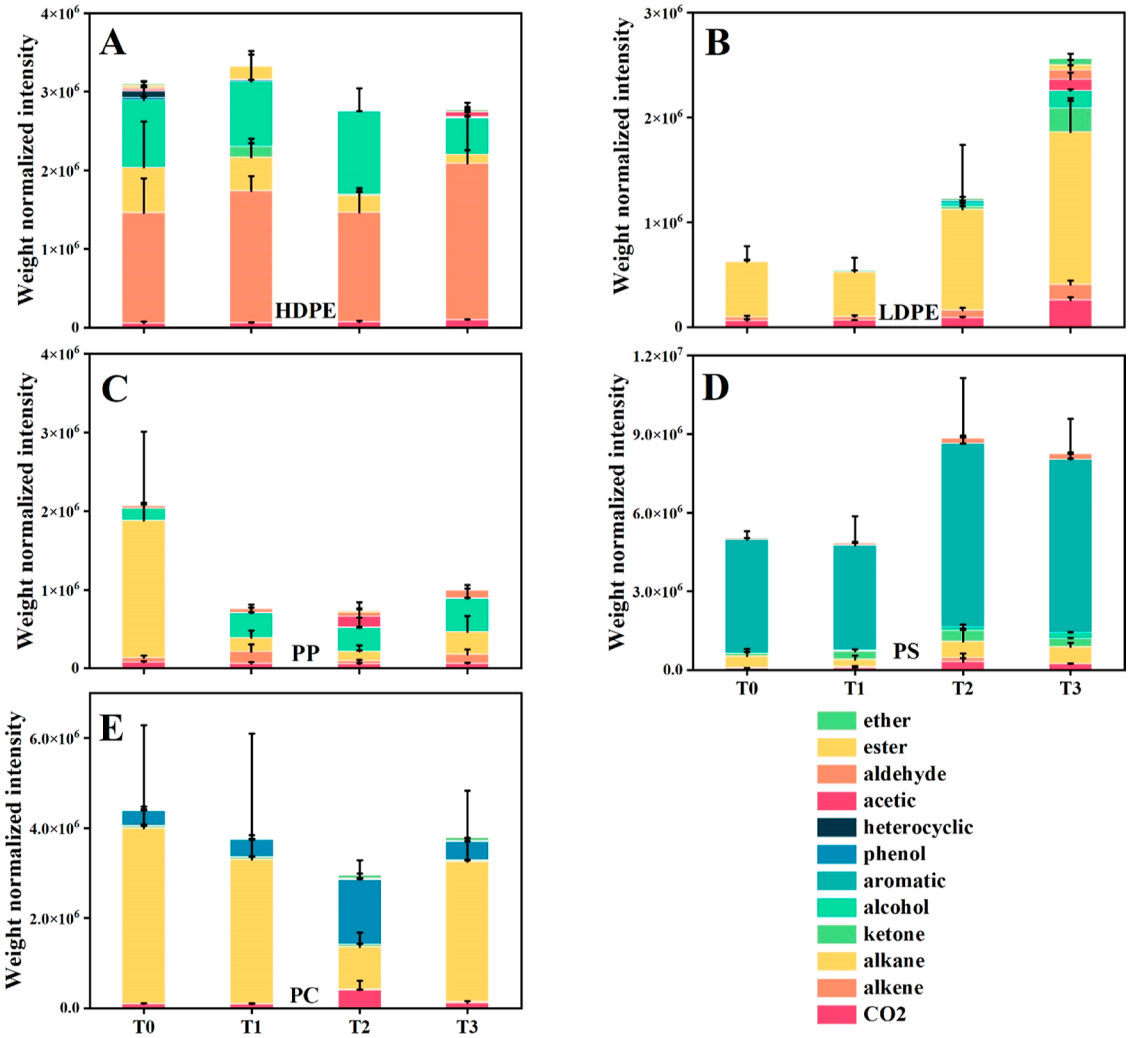

Figure 3. Weight normalized composition of pyrolysis product groups identified through low-temperature pyrolysis of HDPE (A), LDPE (B), PP (C), PS (D), and PC (E) from laboratory weathering experiments. The total peak areas of different chemical classes were normalized by the sample weight. Data are the averages of triplicate normalized peak areas; error bars represent the standard deviations.

chains, leading to chain scission and the formation of shorter, more volatile chains that are more readily detected during pyrolysis.[43] Consistently, it has been observed that oxidized polyethylene yields a higher proportion of lower molecular weight hydrocarbons after simulated photooxidation,[43] although further research is needed for the exact mechanism.

To focus on plastic weathering products and additives, we applied the low temperature mode (350 °C for 0.3 min) of Pyr-GC/MS. In this mode, samples were heated below the T_{onset} of plastics, promoting the preferential release and/or decomposition of additives and weathered products due to their lower molecular weights and bonding energy. Since a much higher temperature is needed to pyrolyze the plastic backbones, this mode also allows a higher amount of sample to be pyrolyzed, thus greatly enhancing the signal/noise ratios of the weathering products and additives. Several additives were identified from the fresh plastics tabs (Figure S1), including bisphenol A in LDPE, butylated hydroxytoluene (BHT) in HDPE, 2,4-di*tert*-butylphenol (2,4-DtBP) in PP, and plasticizer diethyl phthalate in PS. However, these additives were not detectable in every subsample of the same tab, indicating that they were not homogeneously distributed in the plastic polymers. This may explain why the relative intensities of the additives were not constant across the weathering stages. For instance, the intensity of BHT in HDPE samples remained stable at T_1 but decreased at T_2 and T_3, although this change could also be due to the migration of additives during weathering.[44] The heterogeneous distribution or migration of additives during photooxidation would have created different concentrations of additives in plastics, and the absence and/or loss of additives may result in the weakening of the protection from weathering,[44] as well as different physicochemical properties of the plastic surface.

Newly formed compounds from the weathering of plastics were also identified by low-temperature pyrolysis (Figure 3 and Figure S5). To facilitate comparison, these compounds were grouped based on their functional moieties, including alkane, alkene, ketone, alcohol, aromatic, phenol, heterocyclic, acetic, aldehyde, ester, ether groups, and CO_2, based on established protocols.[45] In a semiquantitative way, the different compound groups, excluding the additives aforementioned, were normalized by the sample weight based on their peak heights.

The total intensity of plastic pyrolyzates varied between polymer types and the weathering time. The pyrolyzates of PS had the highest total intensity, while those of other types of plastics shared similar intensities. PS contains a large fraction

https://doi.org/10.1021/acs.est.3c09891
Environ. Sci. Technol. 2024, 58, 14775−14785

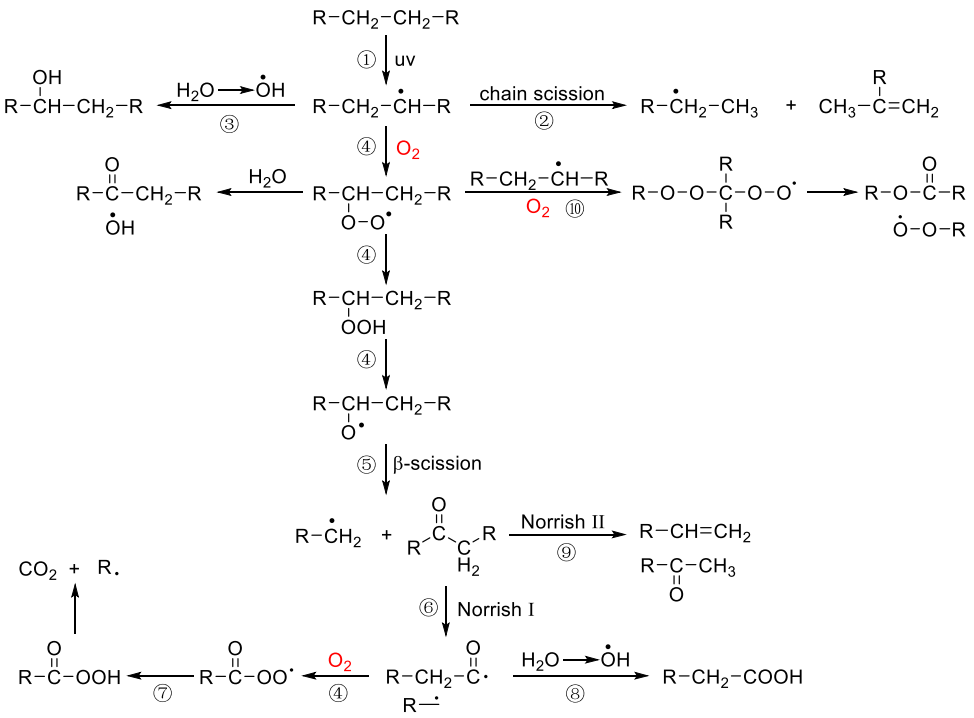

Figure 4. Hypothetical photochemical pathways of plastics under laboratory weathering conditions.

of aromatics, which may have generated more photodegradation products due to their high sensitivity to light. Additionally, given that PS has the lowest TG onset temperatures among all the polymers, around 380 °C (Table 1), which is close to the pyrolysis temperature (350 °C), more pyrolyzates are expected from PS and its weathered products. For example, as much as 3% of PS underwent thermal degradation at this temperature (Table 1). The total intensity of pyrolyzates from HDPE remained constant with time, while those of LDPE and PS increased and those of PC and PP decreased. These trends may be related to a balance between the production of new compounds and their loss to water. For example, the decrease of the pyrolyzates from PC and PP may be due to the loss of photodegradation products to the water due to fragmentation or peeling off of the oxidized surface, an observation consistent with the SEM results (Figure 2).

The pyrolysis of fresh plastic tabs mainly produced *n*-alkanes (C_{10}−C_{24} *n*-alkanes for HDPE, C_{14}−C_{29} for LDPE, C_{10}−C_{24} for PP, and C_{20}−C_{32} for PC), with PS producing primarily a styrene monomer and oligomers (dimer and trimer); these compounds likely originated directly from the backbone structures of the plastics. We also found unsaturated compounds, such as alcohols for HDPE and PP, ethers for LDPE, and phenols for PC, as well as CO_2. With increasing weathering time, the content of oxygen-containing compounds increased, while the content of major pyrolyzates from the backbone structure, such as *n*-alkanes, decreased. For example, acetic compounds appeared at T_3 for HDPE, LDPE, and PS, and at T_2 for PP and PC; alcohols in HDPE increased from T_0 to T_2, and in PS they increased from T_0 to T_3. These oxygen-containing compounds likely originated mainly from photooxidation products.

When plotting the major pyrolysis products against the oxidation index (Figures S5 and S6), the contents of major products negatively correlated with their oxidation indices except for PC (the Pearson correlation coefficients were −0.76, −0.99, −0.46, and −0.70 for HDPE, LDPE, PP, and PS, respectively; 0.20 for PC). This correlation indicates that as photodegradation proceeded, more oxygen was incorporated into the plastic structures, shifting the composition of major pyrolyzates. The identification of acetic and ketone compounds at the late weathering stages (T_2 and T_3) also indicated the incorporation of oxygen into plastic structures, such as through chain scission reactions.[4,38] In addition, the pyrolysis results of PC were consistent with the SEM findings, where PC had the highest weathering signal on T_2, indicating that PC underwent a weathering process similar to that of PP. Notably, a prominent weathering signal was observed in PC at T_2, followed by its disappearance, which can be attributed to the loss of the weathered plastic surface. Overall, the low-temperature pyrolysis results provide insights into the extent of plastic weathering and show that pyrolysis can be used as a semiquantitative approach for assessing plastic weathering.

Hypothetical Weathering Mechanisms in the Surface Layers of Macroplastics. Building on the presented results, we propose the following photooxidation pathways for surface layers of different plastics (Figure 4) based on the oxygen-containing compounds identified and oxygen indices from FTIR, as well as on relevant studies.[4,17,19,37,38] Plastic weathering begins with the generation of alkyl radicals upon UV exposure[20] (Figure 4, reaction ①), and the alkyl radicals further undergo *β*-scission, forming vinyl compounds, as indicated by the increase of C═C index from the FTIR results[46] (Figure 4, reaction ②). Alkyl radicals can also react with hydroxyl radicals in water, producing alcohol compounds,[19] as indicated by the increase of alcohol groups of plastic pyrolyzates and R−OH index from the FTIR results (Figure 4, reaction ③). Additionally, alkyl radicals react with O_2, forming peroxy radicals and alkoxy radicals[47] (Figure 4, reaction ④). The unstable peroxy radicals can be decomposed by hydrogen abstraction from the water to form aldehyde and hydroxyl radical[48,49] (Figure 4, reaction ④) or from the

https://doi.org/10.1021/acs.est.3c09891
Environ. Sci. Technol. 2024, 58, 14775−14785

adjacent chain (discussed in reaction 10). Alkoxy radicals further undergo β-scission, generating alkyl radicals and ketone compounds,[50] as shown in the C═O index of FTIR results and the ketone compounds in the plastic pyrolyzates (Figure 4, reaction ⑤). The ketone compounds, following UV exposure, can undergo two Norrish reactions:[51,52] Norrish I reactions produce acyl and alkyl radicals[53] (Figure 4, reaction ⑥), wherein the acyl radicals are oxidized by O_2 and release CO_2 after hydrogen abstraction and chain scission, as shown by the increase of CO_2 in the plastic pyrolyzates (Figure 4, reaction ⑦). Acyl radicals can also combine with hydroxyl radicals from water, forming acetic compounds,[4] which were observed from the acetic groups in plastic pyrolyzates (Figure 4, reaction ⑧). Norrish II reactions generate ketone and vinyl compounds through hydrogen transfer and subsequent β-scission,[54] matching with the FTIR and pyrolyzate results aforementioned (Figure 4, reaction ⑨). Furthermore, peroxyl radicals combine with alkyl radicals[55] and oxidize to form ketone and ester compounds, which was observed from the ketone and ester groups in plastic pyrolyzates (Figure 4, reaction 10). Overall, the increasing C═C and C═O signals during weathering indicate the prevalence of chain scissions induced by Norrish II reactions. The dominance of R−OH groups after weathering suggests that water played an important role in plastic weathering, providing hydroxyl radicals that fuel chain reactions, different from plastic weathering in air environments.[19] The diffusion of oxygen from water to plastics may have also been more constrained than that in the air environment, potentially inhibiting chain reactions that rely on the availability of oxygen.

Overall Resistance of Macroplastics to Photodegradation. Despite the pronounced oxidation observed in the surface layer, the inner part of the plastics remained nearly intact after an equivalent of 25−75 years of natural UVA irradiation. This resistance could be attributed to the thickness of the plastic tabs (1.6 mm) and the additives present. Oxygen penetration is limited to a thin surface layer,[3] typically a few hundred micrometers, which varies by the polymer type.[56−58] Given the thickness of our plastic tabs, oxygen diffusion into the interior should be minimal. Most studies use plastic powder or thin film to assess weathering impacts on plastics, allowing for rapid detection of changes and shorter experiment durations. However, in our study, the thicker plastic tabs with a much lower specific surface area greatly limited the contact of UV light and oxygen from the surface to the inner part of the plastic. For example, when compared to 100 nm spherical particles, the specific surface area of the plastic tabs in this work was 4 orders of magnitude less. This translates to an equivalent of just 1 day of exposure for 100 nm particles, despite 75 years of UVA exposure for the plastic tabs based on the calculation from the surface area and weight, assuming the smooth surface and homogeneity of plastic. Thus, plastic tabs or any macroplastics receive much less UV radiation in terms of their surface area in natural environments.

Moreover, the rate and extent of weathering are influenced by the concentration of oxygen.[3] As the oxygen within the plastic tabs is depleted through the aforementioned photodegradation reactions, additional oxygen needs to diffuse from the surrounding environment for the oxidation to further proceed. However, in our study, plastic tabs were immersed in seawater, which may provide less oxygen compared with air environments. This oxygen diffusion is a "bottleneck" in water environments,[3,58] with oxidation often limited to a thin surface layer, typically on the order of hundreds of micrometers, e.g., for polyolefins.[56,58] This may be particularly true in our study because of the thickness of the plastic tabs. The oxygen limitation appeared to be more pronounced in the later stages of weathering (T_2 and T_3), where a prominent signal of vinyl and alcohol compounds was observed in the FTIR results. Notably, these reactions do not require the presence of oxygen.

Additives may have also contributed to this overall resistance, as several types of antioxidants, including BHT and 2,4-DtBP, were identified, which protect plastics against oxidation. In addition, small amounts of titanium and aluminum were also identified with energy dispersive spectroscopy (EDS) (unpublished data), which may serve as an inorganic pigment or economic flame retardant,[28,59] also increased the opacity of plastic, hindering the penetration of UV.

Consistently, the degradation process of plastic has been generally demonstrated as unidirectional, from the surface toward the center, with more characteristic changes on the surface.[60] Surface degradation makes the plastic more prone to breakage and fragmentation and increases the chances of microplastic generation, especially in the presence of mechanical forces.[3] In addition, the degradation processes of plastics, from macro- to micro- and nanosized particles, are likely an exponentially accelerating process based on the change of the specific surface area with size. From both field surveys and lab simulations, primary plastics shed secondary microplastics exponentially into the surrounding environment, with smaller primary plastics fragmenting faster.[61−63] The plastic tabs, as primary macroplastics, in this work, however, remained nearly intact both physically and chemically after exposure to UVA for up to an estimated equivalent of 75 years, along with mechanical abrasion. Our results demonstrate a much slower rate of photodegradation compared to many other studies, where microsized plastic standards without additives were used.[17,19,64] Furthermore, many types of plastic debris encountered in the coastal regions are single-use bottles, caps, bags, and packaging boxes, which are similar to the analyzed materials here.[65,66] Despite experiencing natural weathering, these macroplastics may exhibit an extended residence time and a slow degradation process.

Environmental Implications. The results of this work demonstrated that photodegradation in water environments predominantly occurred in the surface layer of macroplastics, with minimal impact on the bulk plastic properties after an equivalent of 25−75 years of UVA irradiation. Different types of plastic share similar radical chain reactions, such as Norrish reactions and hydroxy formation. However, the plastic types exhibited varying susceptibilities to weathering, which can be attributed to their specific chemical composition. Weathering resulted in the incorporation of oxygen into the plastic surface and the loss of the weathered surface to ambient environments. To our best knowledge, this study is the first to categorize plastic pyrolyzates into different chemical groups and to further use their relative quantities to indicate the weathering status of plastics. Overall, this work highlights the importance of size, morphology, and additives in determining the extent of weathering, thus cautioning the generalized extrapolation of laboratory results to the environment. Further research should encompass a broader range of plastic types, including textiles, with different properties and sizes, to accurately estimate plastic weathering in the marine environment.

https://doi.org/10.1021/acs.est.3c09891
Environ. Sci. Technol. 2024, 58, 14775−14785

■ ASSOCIATED CONTENT

Supporting Information

The Supporting Information is available free of charge at https://pubs.acs.org/doi/10.1021/acs.est.3c09891.

Method for high temperature pyrolysis, results for additive analysis, additive concentrations, FTIR spectra, total ion intensity spectra of high temperature pyrolysis, relative composition of pyrolysis product groups, and major chemical classes of pyrolyzates depicted by the oxidation index (PDF)

■ AUTHOR INFORMATION

Corresponding Author

Zhanfei Liu − *The University of Texas at Austin—Marine Science Institute, Port Aransas, Texas 78373, United States;* orcid.org/0000-0002-8897-0698; Email: zhanfei.liu@utexas.edu

Authors

Xiangtao Jiang − *The University of Texas at Austin—Marine Science Institute, Port Aransas, Texas 78373, United States*

Scott Gallager − *Coastal Ocean Vision, North Falmouth, Massachusetts 02556, United States*

Rut Pedrosa Pàmies − *The Ecosystems Center, Marine Biological Laboratory, Woods Hole, Massachusetts 02543, United States;* orcid.org/0000-0003-3504-4727

S. Emil Ruff − *The Ecosystems Center, Marine Biological Laboratory, Woods Hole, Massachusetts 02543, United States*

Complete contact information is available at: https://pubs.acs.org/10.1021/acs.est.3c09891

Notes

The authors declare no competing financial interest.

■ ACKNOWLEDGMENTS

We thank Campos, Daniel S, and Dr. Elizabeth Catlos for their help with the low-vacuum scanning electron microscope. We also thank Dr. Alexander Bochdansky for his help with editing the manuscript and Chase Glatz for his help with SEM−EDS analysis. This work was supported by the National Science Foundation (#2033828) and the Simons Foundation (824763, S.E.R.).

■ REFERENCES

(1) Worm, B.; Lotze, H. K.; Jubinville, I.; Wilcox, C.; Jambeck, J. Plastic as a Persistent Marine Pollutant. *Annu. Rev. Environ. Resour.* **2017**, *42* (1), 1−26.

(2) Kaandorp, M. L. A.; Lobelle, D.; Kehl, C.; Dijkstra, H. A.; van Sebille, E. Global Mass of Buoyant Marine Plastics Dominated by Large Long-Lived Debris. *Nat. Geosci.* **2023**, *16* (8), 689−694.

(3) Andrady, A. L. Weathering and Fragmentation of Plastic Debris in the Ocean Environment. *Mar. Pollut. Bull.* **2022**, *180*, 113761.

(4) Grause, G.; Chien, M.-F.; Inoue, C. Changes during the Weathering of Polyolefins. *Polym. Degrad. Stab.* **2020**, *181*, 109364.

(5) Alimi, O. S.; Claveau-Mallet, D.; Kurusu, R. S.; Lapointe, M.; Bayen, S.; Tufenkji, N. Weathering Pathways and Protocols for Environmentally Relevant Microplastics and Nanoplastics: What Are We Missing? *J. Hazard. Mater.* **2022**, *423*, 126955.

(6) Messinetti, S.; Mercurio, S.; Parolini, M.; Sugni, M.; Pennati, R. Effects of Polystyrene Microplastics on Early Stages of Two Marine Invertebrates with Different Feeding Strategies. *Environ. Pollut.* **2018**, *237*, 1080−1087.

(7) Ahmadifar, E.; Kalhor, N.; Dawood, M. A. O.; Ahmadifar, M.; Moghadam, M. S.; Abarghouei, S.; Hedayati, A. Effects of Polystyrene Microparticles on Inflammation, Antioxidant Enzyme Activities, and Related Gene Expression in Nile Tilapia (Oreochromis Niloticus). *Environ. Sci. Pollut. Res.* **2021**, *28*, 14909−14916.

(8) Li, B.; Ding, Y.; Cheng, X.; Sheng, D.; Xu, Z.; Rong, Q.; Wu, Y.; Zhao, H.; Ji, X.; Zhang, Y. Polyethylene Microplastics Affect the Distribution of Gut Microbiota and Inflammation Development in Mice. *Chemosphere* **2020**, *244*, 125492.

(9) Marana, M. H.; Poulsen, R.; Thormar, E. A.; Clausen, C. G.; Thit, A.; Mathiessen, H.; Jaafar, R.; Korbut, R.; Hansen, A. M. B.; Hansen, M.; Limborg, M. T.; Syberg, K.; von Gersdorff Jørgensen, L. Plastic Nanoparticles Cause Mild Inflammation, Disrupt Metabolic Pathways, Change the Gut Microbiota and Affect Reproduction in Zebrafish: A Full Generation Multi-Omics Study. *J. Hazard. Mater.* **2022**, *424*, 127705.

(10) Jiang, X.; Tian, L.; Ma, Y.; Ji, R. Quantifying the Bioaccumulation of Nanoplastics and PAHs in the Clamworm Perinereis Aibuhitensis. *Sci. Total Environ.* **2019**, *655*, 591−597.

(11) Athey, S. N.; Albotra, S. D.; Gordon, C. A.; Monteleone, B.; Seaton, P.; Andrady, A. L.; Taylor, A. R.; Brander, S. M. Trophic Transfer of Microplastics in an Estuarine Food Chain and the Effects of a Sorbed Legacy Pollutant. *Limnol. Oceanogr. Lett.* **2020**, *5*, 154−162.

(12) Setälä, O.; Fleming-Lehtinen, V.; Lehtiniemi, M. Ingestion and Transfer of Microplastics in the Planktonic Food Web. *Environ. Pollut.* **2014**, *185*, 77−83.

(13) Chen, C.-F.; Ju, Y.-R.; Lim, Y. C.; Chen, C.-W.; Dong, C.-D. Seasonal Variation of Diversity, Weathering, and Inventory of Microplastics in Coast and Harbor Sediments. *Sci. Total Environ.* **2021**, *781*, 146610.

(14) Du, H.; Ma, H.; Xing, B. Identification of Naturally Weathering Microplastics and Their Interactions with Ion Dyes in Aquatic Environments. *Mar. Pollut. Bull.* **2022**, *174*, 113186.

(15) Liu, P.; Zhan, X.; Wu, X.; Li, J.; Wang, H.; Gao, S. Effect of Weathering on Environmental Behavior of Microplastics: Properties, Sorption and Potential Risks. *Chemosphere* **2020**, *242*, 125193.

(16) Turner, A.; Arnold, R.; Williams, T. Weathering and Persistence of Plastic in the Marine Environment: Lessons from LEGO. *Environ. Pollut.* **2020**, *262*, 114299.

(17) Brandon, J.; Goldstein, M.; Ohman, M. D. Long-Term Aging and Degradation of Microplastic Particles: Comparing in Situ Oceanic and Experimental Weathering Patterns. *Mar. Pollut. Bull.* **2016**, *110* (1), 299−308.

(18) Jiang, X.; Lu, K.; Tunnell, J. W.; Liu, Z. The Impacts of Weathering on Concentration and Bioaccessibility of Organic Pollutants Associated with Plastic Pellets (Nurdles) in Coastal Environments. *Mar. Pollut. Bull.* **2021**, *170*, 112592.

(19) Tian, L.; Chen, Q.; Jiang, W.; Wang, L.; Xie, H.; Kalogerakis, N.; Ma, Y.; Ji, R. A Carbon-14 Radiotracer-Based Study on the Phototransformation of Polystyrene Nanoplastics in Water versus in Air. *Environ. Sci.: Nano* **2019**, *6* (9), 2907−2917.

(20) Rånby, B. Photodegradation and Photo-Oxidation of Synthetic Polymers. *J. Anal. Appl. Pyrolysis* **1989**, *15*, 237−247.

(21) Gewert, B.; Plassmann, M.; Sandblom, O.; MacLeod, M. Identification of Chain Scission Products Released to Water by Plastic Exposed to Ultraviolet Light. *Environ. Sci. Technol. Lett.* **2018**, *5*, 272−276.

(22) Shi, Y.; Liu, P.; Wu, X.; Shi, H.; Huang, H.; Wang, H.; Gao, S. Insight into Chain Scission and Release Profiles from Photodegradation of Polycarbonate Microplastics. *Water Res.* **2021**, *195*, 116980.

(23) Gardette, M.; Perthue, A.; Gardette, J.-L.; Janecska, T.; Földes, E.; Pukánszky, B.; Therias, S. Photo- and Thermal-Oxidation of Polyethylene: Comparison of Mechanisms and Influence of Unsaturation Content. *Polym. Degrad. Stab.* **2013**, *98* (11), 2383−2390.

(24) Song, Y. K.; Hong, S. H.; Eo, S.; Han, G. M.; Shim, W. J. Rapid Production of Micro- and Nanoplastics by Fragmentation of

Expanded Polystyrene Exposed to Sunlight. *Environ. Sci. Technol.* **2020**, *54*, 11191−11200.
(25) Song, Y. K.; Hong, S. H.; Jang, M.; Han, G. M.; Jung, S. W.; Shim, W. J. Combined Effects of UV Exposure Duration and Mechanical Abrasion on Microplastic Fragmentation by Polymer Type. *Environ. Sci. Technol.* **2017**, *51* (8), 4368−4376.
(26) Chen, X.; Xu, M.; Yuan, L.; Huang, G.; Chen, X.; Shi, W. Degradation Degree Analysis of Environmental Microplastics by Micro FT-IR Imaging Technology. *Chemosphere* **2021**, *274*, 129779.
(27) Sun, Y.; Yuan, J.; Zhou, T.; Zhao, Y.; Yu, F.; Ma, J. Laboratory Simulation of Microplastics Weathering and Its Adsorption Behaviors in an Aqueous Environment: A Systematic Review. *Environ. Pollut.* **2020**, *265*, 114864.
(28) Walsh, A. N.; Reddy, C. M.; Niles, S. F.; McKenna, A. M.; Hansel, C. M.; Ward, C. P. Plastic Formulation Is an Emerging Control of Its Photochemical Fate in the Ocean. *Environ. Sci. Technol.* **2021**, *55* (18), 12383−12392.
(29) Jahnke, A.; Arp, H. P. H.; Escher, B. I.; Gewert, B.; Gorokhova, E.; Kühnel, D.; Ogonowski, M.; Potthoff, A.; Rummel, C.; Schmitt-Jansen, M.; Toorman, E.; MacLeod, M. Reducing Uncertainty and Confronting Ignorance about the Possible Impacts of Weathering Plastic in the Marine Environment. *Environ. Sci. Technol. Lett.* **2017**, *4* (3), 85−90.
(30) Bottino, F. A.; Cinquegrani, A. R.; Di Pasquale, G.; Leonardi, L.; Pollicino, A. Chemical Modifications, Mechanical Properties and Surface Photo-Oxidation of Films of Polystyrene (PS). *Polym. Test.* **2004**, *23* (4), 405−411.
(31) Rouillon, C.; Bussiere, P.-O.; Desnoux, E.; Collin, S.; Vial, C.; Therias, S.; Gardette, J.-L. Is Carbonyl Index a Quantitative Probe to Monitor Polypropylene Photodegradation? *Polym. Degrad. Stab.* **2016**, *128*, 200−208.
(32) Geyer, R. A Brief History of Plastics. In *Mare Plasticum-The Plastic Sea: Combatting Plastic Pollution Through Science and Art*; Streit-Bianchi, M., Cimadevila, M., Trettnak, W., Eds.; Springer International Publishing: Cham, 2020; pp 31−47.
(33) Webb, A. R. Ozone Depletion and Changes in Environmental UV-B Radiation. **2000**. 17, 36, .
(34) Gouveia, G. R.; Trindade, G. S.; Nery, L. E. M.; Muelbert, J. H. UVA and UVB Penetration in the Water Column of a South West Atlantic Warm Temperate Estuary and Its Effects on Cells and Fish Larvae. *Estuaries Coasts* **2015**, *38* (4), 1147−1162.
(35) Mecherikunnel, A. T.; Richmond, J. Spectral Distribution of Solar Radiation; NASA-TM-82021, 1980. https://ntrs.nasa.gov/citations/19810016493 (accessed Feb 26, 2024).
(36) Jiang, X.; Conner, N.; Lu, K.; Tunnell, J. W.; Liu, Z. Occurrence, Distribution, and Associated Pollutants of Plastic Pellets (Nurdles) in Coastal Areas of South Texas. *Sci. Total Environ.* **2022**, *842*, 156826.
(37) Diepens, M.; Gijsman, P. Photodegradation of Bisphenol A Polycarbonate. *Polym. Degrad. Stab.* **2007**, *92* (3), 397−406.
(38) Yamada, K.; Kumagai, S.; Shiratori, T.; Kameda, T.; Saito, Y.; Watanabe, A.; Watanabe, C.; Teramae, N.; Yoshioka, T. Combined UV-Irradiation and Pyrolysis-GC/MS Approach for Evaluating the Deterioration Behavior of Ethylene Vinyl Acetate. *Polym. Degrad. Stab.* **2021**, *190*, 109623.
(39) Küpper, L.; Gulmine, J. V.; Janissek, P. R.; Heise, H. M. Attenuated Total Reflection Infrared Spectroscopy for Micro-Domain Analysis of Polyethylene Samples after Accelerated Ageing within Weathering Chambers. *Vib. Spectrosc.* **2004**, *34* (1), 63−72.
(40) Toapanta, T.; Okoffo, E. D.; Ede, S.; O'Brien, S.; Burrows, S. D.; Ribeiro, F.; Gallen, M.; Colwell, J.; Whittaker, A. K.; Kaserzon, S.; Thomas, K. V. Influence of Surface Oxidation on the Quantification of Polypropylene Microplastics by Pyrolysis Gas Chromatography Mass Spectrometry. *Sci. Total Environ.* **2021**, *796*, 148835.
(41) Philippart, J.-L.; Posada, F.; Gardette, J.-L. Mass Spectroscopy Analysis of Volatile Photoproducts in Photooxidation of Polypropylene. *Polym. Degrad. Stab.* **1995**, *49* (2), 285−290.
(42) Bonijoly, M.; Oberlin, M.; Oberlin, A. A Possible Mechanism for Natural Graphite Formation. *Int. J. Coal Geol.* **1982**, *1* (4), 283−312.
(43) Biale, G.; La Nasa, J.; Mattonai, M.; Corti, A.; Vinciguerra, V.; Castelvetro, V.; Modugno, F. A Systematic Study on the Degradation Products Generated from Artificially Aged Microplastics. *Polymers* **2021**, *13* (12), 1997.
(44) Yang, R.; Zhao, J.; Liu, Y. Oxidative Degradation Products Analysis of Polymer Materials by Pyrolysis Gas Chromatography-Mass Spectrometry. *Polym. Degrad. Stab.* **2013**, *98* (12), 2466−2472.
(45) Lu, K.; Xue, J.; Guo, L.; Liu, Z. The Bio- and Thermal Lability of Dissolved Organic Matter as Revealed by High-Resolution Mass Spectrometry and Thermal Chemical Analyses. *Mar. Chem.* **2023**, *250*, 104184.
(46) Rajakumar, K.; Sarasvathy, V.; Thamarai Chelvan, A.; Chitra, R.; Vijayakumar, C. T. Natural Weathering Studies of Polypropylene. *J. Polym. Environ.* **2009**, *17* (3), 191−202.
(47) Osawa, Z.; Someya, M.; Fu, Y. S.; Konoma, F. Studies of Chemiluminescence Observed in Photo-Irradiated and Weathered Polypropylene in the Early Stages. *Polym. Degrad. Stab.* **1994**, *43* (3), 461−470.
(48) Yousif, E.; Haddad, R. Photodegradation and Photostabilization of Polymers, Especially Polystyrene: Review. *SpringerPlus* **2013**, *2* (1), 398.
(49) Rabek, J. F. Photodegradation and Photo-Oxidative Degradation of Homochain Polymers. In *Polymer Photodegradation: Mechanisms and Experimental Methods*; Rabek, J. F., Ed.; Springer Netherlands: Dordrecht, 1995; pp 67−254.
(50) Tidjani, A. Photooxidation of Polypropylene under Natural and Accelerated Weathering Conditions. *J. Appl. Polym. Sci.* **1997**, *64* (13), 2497−2503.
(51) Stark, N. M.; Matuana, L. M. Surface Chemistry Changes of Weathered HDPE/Wood-Flour Composites Studied by XPS and FTIR Spectroscopy. *Polym. Degrad. Stab.* **2004**, *86* (1), 1−9.
(52) Chabira, S. F.; Sebaa, M.; G'sell, C. Influence of Climatic Ageing on the Mechanical Properties and the Microstructure of Low-Density Polyethylene Films. *J. Appl. Polym. Sci.* **2008**, *110* (4), 2516−2524.
(53) Douminge, L.; Mallarino, S.; Cohendoz, S.; Feaugas, X.; Bernard, J. Extrinsic Fluorescence as a Sensitive Method for Studying Photo-Degradation of High Density Polyethylene Part I. *Curr. Appl. Phys.* **2010**, *10* (4), 1211−1215.
(54) Marsich, L.; Ferluga, A.; Cozzarini, L.; Caniato, M.; Sbaizero, O.; Schmid, C. The Effect of Artificial Weathering on PP Coextruded Tape and Laminate. *Composites, Part A* **2017**, *95*, 370−376.
(55) Tidjani, A.; Arnaud, R. Photo-Oxidation of Linear Low Density Polyethylene: A Comparison of Photoproducts Formation under Natural and Accelerated Exposure. *Polym. Degrad. Stab.* **1993**, *39* (3), 285−292.
(56) Shyichuk, A. V.; Turton, T. J.; White, J. R.; Syrotynska, I. D. Different Degradability of Two Similar Polypropylenes as Revealed by Macromolecule Scission and Crosslinking Rates. *Polym. Degrad. Stab.* **2004**, *86* (2), 377−383.
(57) Nagai, N.; Matsunobe, T.; Imai, T. Infrared Analysis of Depth Profiles in UV-Photochemical Degradation of Polymers. *Polym. Degrad. Stab.* **2005**, *88* (2), 224−233.
(58) Andrady, A. L.; Lavender-Law, K.; Donohue, J.; Koongolla, B. Accelerated Degradation of Low-Density Polyethylene in Air and in Sea Water. *Sci. Total Environ.* **2022**, *811*, 151368.
(59) Bautista, T. O. Aluminum Trihydrate: A Powerful Additive for Track and Flame Retardancy of Reinforced Plastics. *Polym.-Plast. Technol. Eng.* **1982**, *18* (2), 179−207.
(60) Chamas, A.; Moon, H.; Zheng, J.; Qiu, Y.; Tabassum, T.; Jang, J. H.; Abu-Omar, M. M.; Scott, S. L.; Suh, S. Degradation Rates of Plastics in the Environment. *ACS Sustainable Chem. Eng.* **2020**, *8*, 3494−3511.
(61) Pramanik, B. K.; Pramanik, S. K.; Monira, S. Understanding the Fragmentation of Microplastics into Nano-Plastics and Removal of

https://doi.org/10.1021/acs.est.3c09891
Environ. Sci. Technol. 2024, 58, 14775−14785

Nano/Microplastics from Wastewater Using Membrane, Air Flotation and Nano-Ferrofluid Processes. *Chemosphere* **2021**, *282*, 131053.
(62) Efimova, I.; Bagaeva, M.; Bagaev, A.; Chubarenko, I. P.; Chubarenko, I. P. Secondary Microplastics Generation in the Sea Swash Zone with Coarse Bottom Sediments: Laboratory Experiments. *Front. Mar. Sci.* **2018**, *5*, 313.
(63) Lambert, S.; Wagner, M. Characterisation of Nanoplastics during the Degradation of Polystyrene. *Chemosphere* **2016**, *145*, 265−268.
(64) Ward, C. P.; Armstrong, C. J.; Walsh, A. N.; Jackson, J. H.; Reddy, C. M. Sunlight Converts Polystyrene to Carbon Dioxide and Dissolved Organic Carbon. *Environ. Sci. Technol. Lett.* **2019**, *6*, 669−674.
(65) Law, K. L.; Thompson, R. C. Microplastics in the Seas. *Science* **2014**, *345* (6193), 144−145.
(66) Wessel, C.; Swanson, K.; Weatherall, T.; Cebrian, J. Accumulation and Distribution of Marine Debris on Barrier Islands across the Northern Gulf of Mexico. *Mar. Pollut. Bull.* **2019**, *139*, 14−22.

https://doi.org/10.1021/acs.est.3c09891
Environ. Sci. Technol. 2024, 58, 14775−14785